International Journal of Precision Engineering and Manufacturing (2022) 23:445–451
https://doi.org/10.1007/s12541-022-00628-z

Online ISSN 2005-4602
Print ISSN 2234-7593

REGULAR PAPER

Is Coating Oxide on Porous Metal Thin-Film for Low-Temperature Solid Oxide Fuel Cell Cathode a Panacea for Performance Enhancement?

SangHoon Ji[1] · **WeonJae Kim**[1]

Received: 27 December 2020 / Revised: 11 September 2021 / Accepted: 3 February 2022 / Published online: 25 February 2022

Abstract
The Pt thin-film cathode thermo-mechanically reinforced by using atomic layer-deposited (ALD) alumina overcoat for low-temperature solid oxide fuel cells was investigated on electrochemical and electrical performances and its area specific resistance (ASR) with respect to cell dimension was evaluated. The nanoporous Pt thin-film cathode was fabricated by direct current magnetron sputtering with a deposition pressure of 50 mTorr. And alumina overcoat was deposited with thermal ALD 30 cycles onto the nanoporous Pt thin-film cathode. Compared to bare Pt thin-film cathode, ALD alumina-overcoated Pt thin-film cathode provided ~ 3-times lower activation ASR and ~ 2-times lower effective electrical conductivity after 4-h operation at 550 °C. Despite increases in the thermo-mechanical stability of Pt thin-film cathode by ALD alumina overcoating, it was evaluated that the total ASR of ALD alumina-overcoated Pt thin-film cathode was lower than that of the bare Pt thin-film cathode only if cell dimension is below 0.95 cm^2 because of its lower current collecting performance in the in-plane direction.

Keywords Current collection performance · Alumina overcoat · Pt thin-film cathode · Low-temperature solid oxide fuel cell

1 Introduction

Solid oxide fuel cells (SOFCs) are energy conversion devices to electrochemically produce electrical and heat energy from various chemical fuels such as hydrogen, natural gas, and biogas. Among them, the thin-film-based SOFC (TF-SOFC) capable of generating high power density even below 600 °C is being recognized as a next-generation SOFC type in comparison with conventional SOFCs suffering from a few material and system issues due to extremely high temperature operation above 800 °C [1]. This TF-SOFC can overcome sluggish oxygen reduction reaction (ORR) when metals such as Pt, Pd, or Ag with a nanoporous microstructure are used as electrode-catalyst material on the cathode side; however, the high surface energy of nanoporous metal electrodes causes the microstructural deformation under elevated temperature environments, degrading the catalytic reaction performance of TF-SOFCs [2]. Various solutions to alleviate this electrode stability issue were proposed by many researchers: putting oxide inside the metal electrode and covering oxide overcoat onto the metal electrode are two representative ways.

Atomic layer deposition (ALD) method capable of exhibiting precise thickness controllability at atomic scale and excellent conformality for nano structures has been actively utilized to cover the nanoporous metal electrode with oxide overcoat [3, 4]. Figure 1 shows a concept of ALD oxide overcoating strategy to enhance the thermo-mechanical stability of nanoporous metal cathode. Representatively, Chang et al. covered nanoporous Pt thin-film cathode with an yttria-stabilized zirconia (YSZ) overcoat by ALD and their TF-SOFC presented ~ 2.5-times smaller cathode activation resistance through improvement of thermo-mechanical stability and reaction activity [5]. Liu et al. covered nanoporous Pt thin-film cathode with a zirconia overcoat by ALD and their TF-SOFC generated ~ 10-times higher power density than TF-SOFC with bare nanoporous Pt thin-film cathode [6]. Li et al. showed potential as metal cathode of nanoporous Ag thin film with the help of an ALD YSZ overcoat [7]. Seo

This paper was presented at PRESM2020.

✉ SangHoon Ji
sanghoonji@kict.re.kr

[1] Department of Environmental Research, Korea Institute of Civil Engineering and Building Technology, Goyangdae-Ro 283, Ilsanseo-Gu, Goyang 10223, South Korea

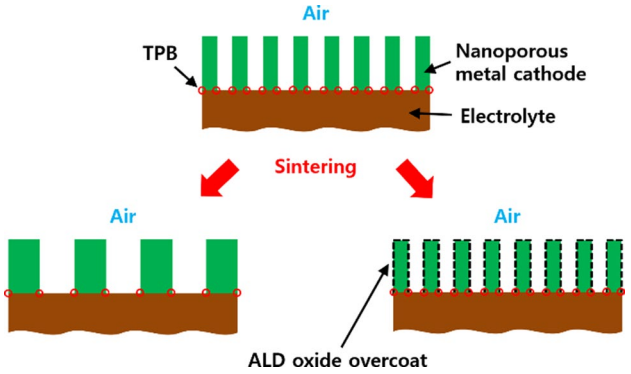

Fig. 1 Schematic diagram describing a strategy to preserve triple phase boundary (TPB) of nanoporous metal cathode by using atomic layer deposition (ALD) oxide overcoat

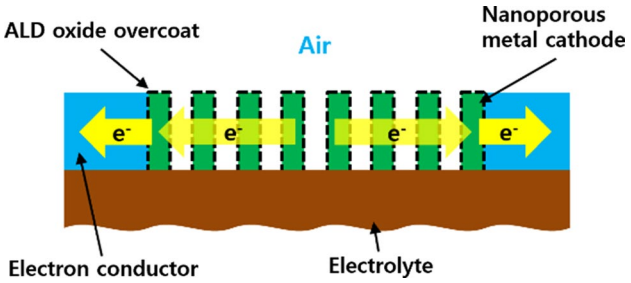

Fig. 2 Schematic diagram describing a methodology to conduct current collection in the in-plane direction

et al. covered nanoporous Pt thin-film cathode with an ALD alumina overcoat and their TF-SOFC presented ~ 2-times smaller cathode activation resistance through improvement of thermo-mechanical stability [8]. Apart from such fuel cell demonstration studies, the mechanism of cathodic performance enhancement by ALD oxide overcoating was elucidated through structural, chemical, and electrochemical characterizations [9, 10].

Even though the effects of an ALD oxide overcoat for nanoporous metal thin-film cathode were discussed thoroughly up to date from other studies, their topic was mainly focused on reaction kinetics than charge transport (i.e., current collection performance associated with electrode is one of the important factors determining ohmic resistance of SOFCs). Contrary to conventional SOFC capable of conducting current collection in the through-plane direction by physical pressing of gas movable, an electronically conductive structure, the TF-SOFC that is highly vulnerable to external forces so that performing current collection in the in-plane direction by contacting an electron conductor to the side of the electrode is favorable as shown in Fig. 2 [11, 12]. This type of current collection methodology can result in a remarkable increase of ohmic resistance with respect to cell dimension; in other words, the area specific resistance augments as cell dimension increases. Therefore, the contribution of current collection performance in large-area TF-SOFCs to generate high output power needs to be examined with carefully.

In this study, the relationship between the reaction kinetics characteristics and the current collecting performance for ALD alumina-overcoated Pt thin-film cathode with a nanoporous microstructure was examined in terms of cell dimension by experimental data-based estimation. First, deposition pressure was selected for fabricating nanoporous Pt thin film. Next, the nanoporous Pt thin film deposited at selected process parameters was overcoated with ALD alumina, which was electrochemically and electrically evaluated. Lastly, activation and ohmic area specific resistances (ASRs) of the ALD alumina-overcoated Pt thin-film cathode were estimated assuming the use of nanogranular electrolyte and particularly their area dependency was investigated. When cell dimension was above 0.95 cm^2, it was evaluated that total ASR of the ALD alumina-overcoated Pt thin-film cathode became larger than that of bare Pt thin-film cathode because of higher ohmic ASR.

2 Method

2.1 Thin-Film Electrode Fabrication

Pt thin films with a nanoporous microstructure were fabricated through direct current magnetron sputtering method (A-Tech System, Korea). A 99.9% purity Pt disk was used as the sputtering target and 99.99% purity Ar was used as the sputtering gas. Target-to-substrate distance was set to 100 mm. Sputtering power was adjusted to 100 W. A double side-polished 8 mol% YSZ single crystal (100) substrate was used as electrolyte for evaluating electrochemical and electrical properties of Pt thin films.

Alumina overcoat was fabricated through ALD method (Atomic Classic, CN1, South Korea). Trimethylaluminium, $Al(CH_3)_3$, and deionized water, H_2O, were used as sources for aluminum and oxygen, respectively. 99.99% purity N_2 was used for both carrier gas and purging gas. The substrate inserted in the ALD chamber was heated to 233 °C. Alumina was deposited by repeating the sequence of Al precursor exposure (0.5 s), Ar gas purge (15 s), H_2O reactant exposure (1 s), and Ar gas purge (15 s). The growth rate of ALD alumina was measured to be 0.12 nm. To fabricate gas-permeable ALD alumina overcoat, ALD cycle numbers were controlled to 30.

2.2 Thin-Film Electrode Characterization

The surface microstructure of thin films was investigated through field emission scanning electron microscopy

(FE-SEM, S-4800, Hitachi, Japan). The spreading resistance of thin films was measured by using a voltage measuring instrument (NI 9206, National Instruments, USA) under ambient air atmosphere at 550˚C.

The cathode activation resistance for the bulk YSZ electrolyte-based two symmetrical cells with a configuration of Pt/YSZ/Pt and alumina-overcoated Pt/YSZ/alumina-overcoated Pt was analyzed by alternating current impedance spectroscopy (VSP-300, Bio-Logic, France). The symmetrical cell configuration is more simple in measuring the activation resistance of one type of electrode than the asymmetrical cell configuration; on the other hand, the interpretation of the voltage-biased data measured with a symmetrical cell configuration is rather complicated. The impedance data of cells operated under open circuit voltage (OCV) was measured with a frequency range of 10 kHz–2 MHz and an alternating current amplitude of 20 mV. Operating environment was controlled with oxygen mole fraction of 0.21 at 550 °C.

3 Results and Discussion

3.1 Deposition Pressure Control to Fabricate Nanoporous Pt Thin Film

Basically, fuel cell electrodes with a highly porous microstructure tend to deliver high electrochemical performance by accelerating reaction kinetics and activating mass transport. We controlled the deposition pressure to fabricate Pt thin films with a nanoporous microstructure. It has been reported that for fuel cell applications, the porosity of Pt thin films deposited by sputtering can be controlled by changing the deposition pressure [13]. Earlier studies showed that Pt thin films deposited below 10 mTorr have high volumetric density [13–15] and therefore Pt thin films with a deposition range of 10 mTorr to 90 mTorr were microstructurally characterized. Figure 3 shows the FE-SEM top view (2a, 2c, and 2e) and cross-sectional view (2b, 2d, and 2f) images for Pt thin films deposited on Si substrates at 10 mTorr, 50 mTorr, and 90 mTorr. Pt thin film deposited at 10 mTorr consists of highly crystalline Pt columns and has no evident voids at nanoscale, while Pt thin film deposited at 50 mTorr consists of less crystalline Pt columns and has relatively clear voids between Pt columns. Four-point probe measurements showed that Pt thin film deposited at 50 mTorr provides effective electrical resistivity of ~ 1,200 Ω-nm which is ~ 10-times higher value than that of Pt thin film deposited at 10 mTorr, meaning its relatively poor connectivity between Pt columns (and/or Pt clusters). Although there was a distinguishable difference in size of Pt columns between Pt thin films deposited at 50 mTorr and 90 mTorr, their effective electrical resistivity values were almost similar. From the fact that weaker adhesive strength between deposit and substrate could incur a higher degree of thermal agglomeration at elevated temperatures, finally the deposition pressure of 50 mTorr was selected for fabricating Pt thin-film cathode with a nanoporous microstructure [16, 17].

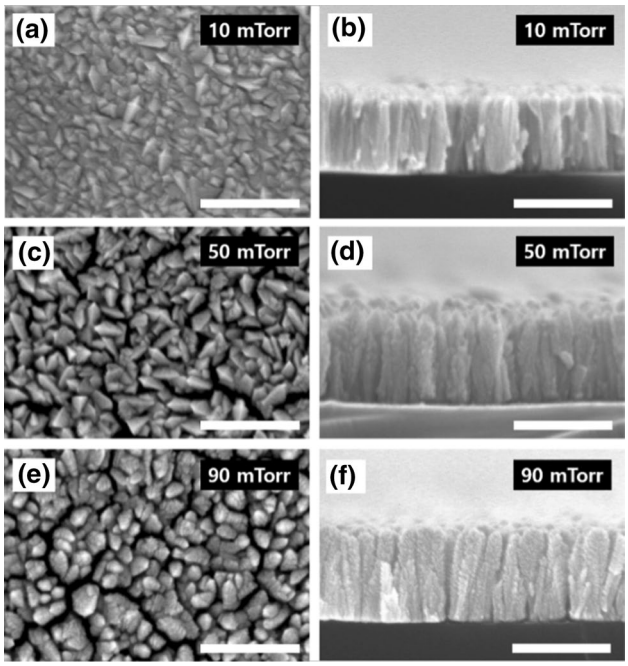

Fig. 3 Field scanning electron microscopy (FE-SEM) top view (**a**, **c**, and **e**) and cross-sectional view (**b**, **d**, and **f**) images for Pt thin films deposited at 10 mTorr, 50 mTorr, and 90 mTorr (scale bar: 200 nm)

3.2 Measurements of Activation ASR and Effective Electrical Conductivity

120-nm-thick bare, nanoporous Pt thin film was covered with ALD alumina overcoat and analyzed its electrochemical and electrical properties under the fuel cell operating environment. Figures 4 and 5 show the cathode activation ASR and the effective electrical conductivity, whose rates of change became below 3%/hr in 4 h. The bare Pt thin-film cathode provided ~ 1.8-times higher initial value of cathode activation ASR than the ALD alumina-overcoated Pt thin-film cathode. It is considered that this behavior is attributed to enhancement of thermo-mechanical stability in consideration of inertness of alumina in terms of catalytic activity [18]. This expectation is underpinned by microscopic imaging results (Fig. 6) which shows a clear difference in surface microstructure between bare Pt thin-film cathode and ALD alumina-overcoated Pt thin-film cathode after 4 h of operation.

The predominant size difference of Pt grains (or Pt columns) for two kinds of electrodes implies that alumina overcoat plays a role in maintaining the length of TPB, which is based on the previous study result that for ALD

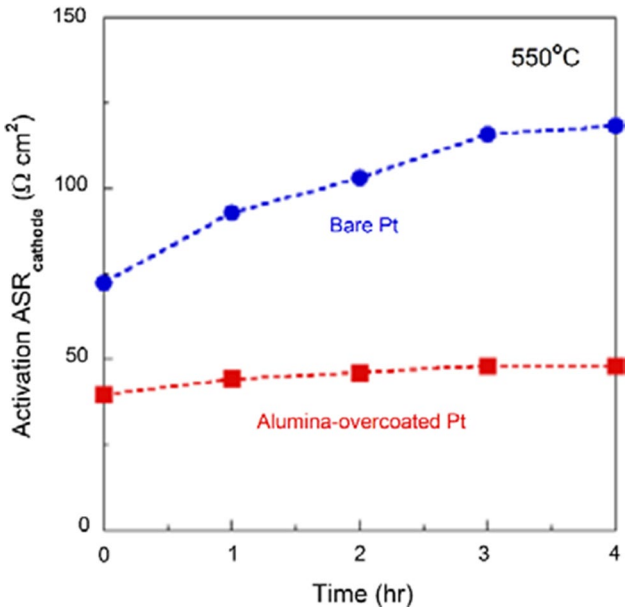

Fig. 4 Cathode activation area specific resistance (ASR) for bare Pt thin film and ALD alumina-overcoated Pt thin film, measured for 4 h at 550 °C

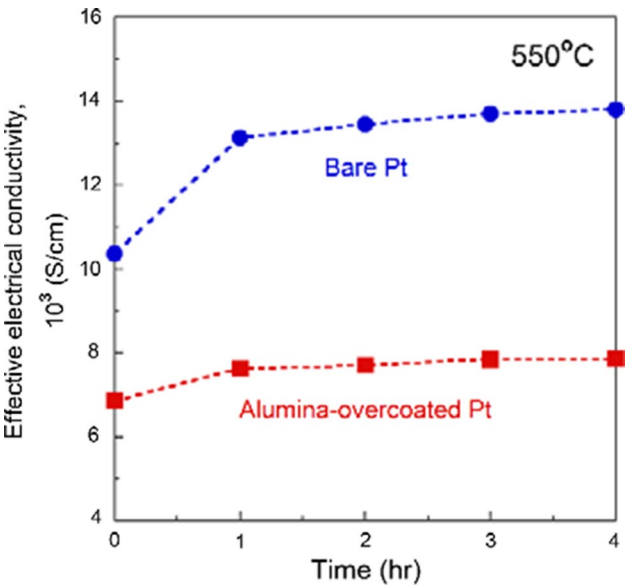

Fig. 5 Effective electrical conductivity for bare Pt thin film and ALD alumina-overcoated Pt thin film, measured for 4 h at 550 °C

alumina-overcoated Pt thin-film cathode the bottom-view microstructure of sintered film in contact with a substrate is also highly porous if the top-view microstructure of sintered film is highly porous [8]. After the operation for 4 h, the bare Pt thin-film cathode provided ~ 3-times higher initial value of cathode activation ASR than the ALD alumina-overcoated

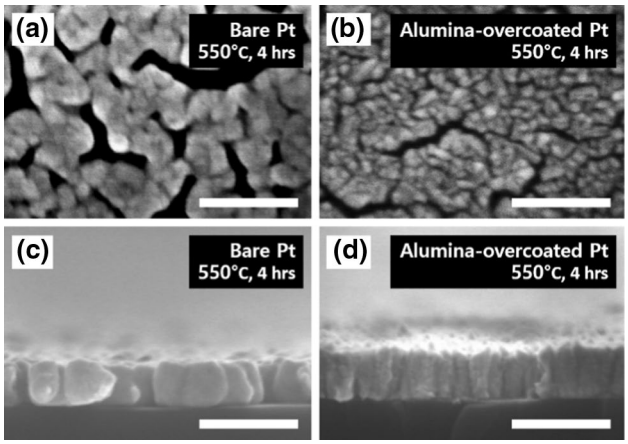

Fig. 6 FE-SEM top view (**a** and **b**) and cross-sectional (**c** and **d**) images for bare Pt thin film and ALD alumina-overcoated Pt thin film, heated for 4 h at 550 °C (scale bar: 200 nm)

Pt thin-film cathode. For metal thin films, the path of electrons is reduced due to severe aggregation of individual metal particles if the temperature is too high, whereas below a certain temperature, the growth of individual metal particles mainly occurs and electron transport resistance tends to decrease [12, 19]. This result suggests that ALD alumina overcoat plays a role as the effective inhibitor preventing nanoporous Pt thin film with high surface energy from agglomerating. The effective electrical conductivity of Fig. 5 was obtained in consideration of spreading resistance and geometrical information. The bare Pt thin-film cathode provided ~ 1.5-times higher initial value of effective electrical conductivity than the ALD alumina-overcoated Pt thin-film cathode. This lower effective electrical conductivity of ALD alumina-overcoated Pt thin-film cathode with higher thermo-mechanical stability is probably because of its lower degree of physical connectivity between individual Pt columns.

After the operation for 4 h, the bare Pt thin-film cathode provided ~ 2-times higher effective electrical conductivity than the ALD alumina-overcoated Pt thin-film cathode. This result implies that applying ALD alumina overcoat to nanoporous Pt thin-film cathode might not be a spanacea for generating high-performance of TF-SOFCs operated at low temperatures.

3.3 ASR Estimation for ALD Electrolyte-Embedded TF-SOFC

The analysis of electrochemical and electrical characteristics for electrode-catalysts investigated in this study were conducted using bulk YSZ electrolyte with considerably large grains (or low grain boundary density). However, electrolytes fabricated by vapor deposition techniques (e.g., sputtering, chemical vapor deposition, and ALD) frequently used

in fabrication of actual TF-SOFCs have very small grains (or high grain boundary density) [1]. For instance, it is generally known that ALD-prepared electrolytes have grains with a size of a few tens of nanometers and therefore fast reaction kinetics at the electrode–electrolyte interface is achievable due to their very high grain boundary density [20, 21]. While the reaction characteristics on the surface of the electrolyte produced by typical high-temperature sintering process can be greatly changed mainly through changes in composition and microstructure, in the electrolyte produced at relatively low temperatures through the ALD process, grain boundary density can have an impact on reaction characteristics in addition to above-mentioned factors. From Fig. 7 showing schematically such a difference in grain size of YSZ electrolyte, it is recognizable that ALD YSZ electrolyte nanoporous Pt thin-film cathode could present much more electrolyte grain boundary-cathode meeting points than bulk YSZ electrolyte. By assuming the use of ALD YSZ thin-film electrolyte, activation ASRs for Pt thin-film cathode and ALD alumina-overcoated Pt thin-film cathode were estimated based on the measurement data obtained from the previous section. The following two experimental, empirical grounds for estimating activation ASR are considered. The first consideration of estimation is that very thin ALD YSZ electrolyte is capable of providing ~ 10-times smaller cathode reaction kinetics compared to bulk YSZ [21, 22]. The second consideration of estimation is that for Pt/YSZ/Pt cell configuration, cathode activation resistance measured in the current density region providing the maximal power density is ~ 5-times smaller than cathode activation resistance measured under OCV [23–25]. The authors believe that this assumption is sufficiently valid from the experimental results

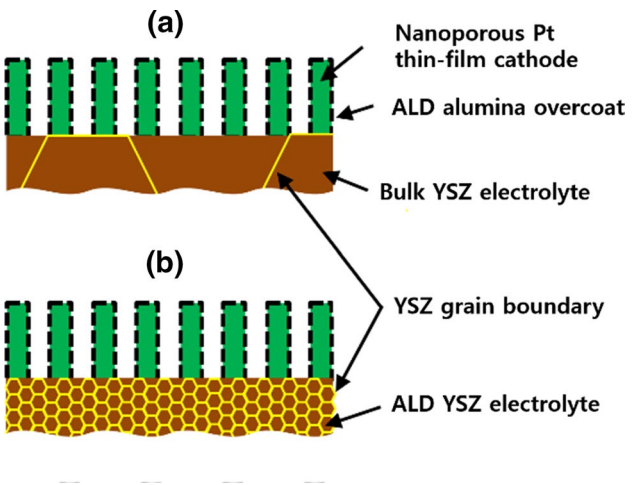

Fig. 7 Schematic of ALD alumina-overcoated Pt thin-film cathode deposited on **a** bulk yttria-stabilized zirconia (YSZ) electrolyte with low grain boundary density and **b** ALD YSZ electrolyte with much higher grain boundary density

of other researchers that the polarization curve analysis of TF-SOFC with the same configuration of electrolyte and electrode shows that the resistance at the voltage regime providing maximum power density (~ 0.73 Ω cm^2) is ~ 5-times smaller than the resistance at OCV (~ 3.72 Ω-cm^2) [23]. From these two considerations, it is expectable that ALD YSZ electrolyte will provide ~ 50-times smaller cathode activation ASR in the current density region providing the maximal power density compared to bulk YSZ electrolyte. As a result, it is expected that the cathode activation ASRs for bare Pt thin-film cathode and ALD alumina-overcoated Pt thin-film cathode through 4-h operation at 550 °C will reach ~ 2.37 Ω cm^2 and ~ 0.96 Ω cm^2, respectively. Because activation ASR studied in this study is continuous regardless of cell dimension, its variation with respect to cell dimension can be plotted as shown in Fig. 8a [19]. Meanwhile, there was little difference in the change rate of sheet resistance of 120-nm-thick nanoporous Pt thin films, deposited on a bulk YSZ substrate and a ~ 100-nm-thick ALD YSZ-coated YSZ substrate, heated 4 h at 550 °C. Thus, it can be considered that the kind of the YSZ electrolyte (the grain size of YSZ electrolyte) has little impact on the time variation of effective electrical conductivity through 4-h operation at 550 °C. Contrary to activation ASR, ohmic ASR investigated in this study increases by an increase in cell dimension because of the dominative in-plan conduction of electrons. Therefore, its variation with respect to cell dimension can be plotted as shown in Fig. 8b. Total ASR values by adding activation ASR values to ohmic ASR values can be plotted as shown in Fig. 8c and there appeared an intersection point of cell dimension of 0.95 cm^2. This result shows that ALD alumina-overcoated Pt thin-film cathode provides a relatively higher cathode ASR than bare Pt thin-film cathode when cell dimension is above 0.95 cm^2. Eventually, it is considered that ALD alumina-overcoated Pt thin-film cathode could generate insufficient power density due to its high change transport resistance even though ALD alumina overcoat acts as a supporter to maintain robustness of nanoporous Pt thin-film cathode.

4 Concluding Remarks

The noble metal thin-film cathode, thermo-mechanically stabilized by overcoating of ALD oxide, used as cathode for low-temperature SOFCs, was rationally designed in consideration of activation and ohmic ASRs and eventually one finding was obtained from this study. The finding is that ALD oxide overcoat used as the inhibitor preventing nanoporous noble metal thin-film cathode from deforming cannot be a panacea for fabricating high-performance low-temperature SOFC cathode; this is because ALD oxide overcoating incurs relatively low current collecting performance in spite

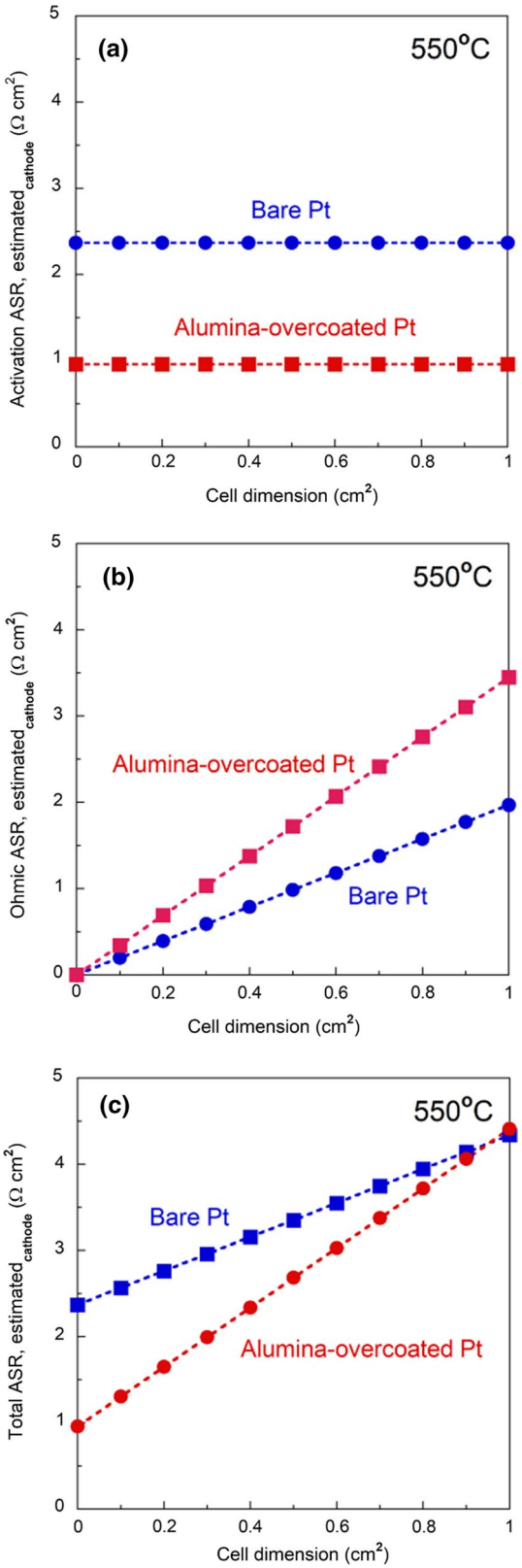

Fig. 8 Estimation of cathode ASRs with respect to cell dimension for bare Pt thin-film cathode and ALD alumina-overcoated Pt thin-film cathode: **a** activation ASR, **b** ohmic ASR, and **c** total ASR (the sum of activation ASR and ohmic ASR), at 550 °C

of its thermo-mechanically stabilizing effects. Furthermore, because cell dimension needs to enlarge as soon as possible for providing high output power, stacking an additional current collecting thin film could be an attractive solution to fabricate low-temperature SOFC cathode providing sufficiently high current collecting performance.

Acknowledgements This work was supported by the National Research Foundation of Korea Project (No. NRF-2018R1D1A1B07048082) and the Korea Institute of Civil Engineering and Building Technology Project (No. 20210154, 20210524). The authors would like to thank Professor WooChul Jung at Korea Advanced Institute of Science and Technology for sharing experimental infrastructure.

References

1. Lee, Y. H., Chang, I., Cho, G. Y., Park, J., Yu, W., Tanveer, W. H., & Cha, S. W. (2018). Thin film solid oxide fuel cells operating below 600°C: A review. *International Journal of Precision Engineering and Manufacturing-Green Technology, 5*(3), 441–453.
2. Ji, S., Chang, I., Cho, G. Y., Lee, Y. H., Shim, J. H., & Cha, S. W. (2014). Application of dense nano-thin platinum films for low-temperature solid oxide fuel cells by atomic layer deposition. *International Journal of Hydrogen Energy, 39*(23), 12402–12408.
3. Seo, J., Tsvetkov, N., Jeong, S. J., Yoo, Y., Ji, S., Kim, J. H., Kang, J. K., & Jung, W. (2020). Gas-permeable inorganic shell improves the coking stability and electrochemical reactivity of Pt toward methane oxidation. *ACS Applied Materials & Interfaces, 14*(4), 4405–4413.
4. Karimaghaloo, A., Koo, J., Kang, H. S., Song, S. A., Shim, J. H., & Lee, M. H. (2019). Nanoscale surface and interface engineering of solid oxide fuel cells by atomic layer deposition. *International Journal of Precision Engineering and Manufacturing-Green Technology, 6*, 611–628.
5. Chang, I., Ji, S., Park, J., Lee, M. H., & Cha, S. W. (2015). Ultrathin YSZ coating on Pt cathode for high thermal stability and enhanced oxygen reduction reaction activity. *Advanced Energy Materials, 5*(10), 1402251.
6. Liu, K.-Y., Fan, L., Yu, C.-C., & Su, P.-C. (2008). Thermal stability and performance enhancement of nano-porous platinum cathode in solid oxide fuel cells by nanoscale ZrO_2 capping. *Electrochemistry Communications, 56*, 65–69.
7. Li, Y. K., Choi, H. J., Kim, H. K., Chean, N. K., Kim, M., Koo, J., Jeong, H. J., Jang, D. Y., & Shim, J. H. (2015). Nanoporous silver cathodes surface-treated by atomic layer deposition of Y:ZrO_2 for high-performance low-temperature solid oxide fuel cells. *Journal of Power Sources, 295*, 175–181.
8. Seo, H. G., Ji, S., Seo, J., Kim, S., Koo, B., Choi, Y., Kim, H., Kim, J. H., Kim, T. S., & Jung, W. (2020). Sintering-resistant platinum electrode achieved through atomic layer deposition for thin-film solid oxide fuel cells. *Journal of Alloys and Compounds, 835*(15), 155347.
9. Li, H., Kang, H. S., Grewal, S., Nelson, A. J., Song, S. A., & Lee, M. H. (2020). How an Angstrom-thick oxide overcoat enhances durability and activity of nanoparticle-decorated cathodes in solid oxide fuel cells. *Journal of Materials Chemistry A, 8*, 15927.
10. Karimaghaloo, A., Andrade, A. M., Grewal, S., Shim, J. H., & Lee, M. H. (2016). Mechanism of cathodic performance enhancement by a few-nanometer-thick oxide overcoat on porous Pt cathodes of solid oxide fuel cells. *ACS Omega, 2*, 806–813.
11. Chang, I., Bae, J., Park, J., Lee, S., Ban, M., Park, T., Lee, Y. H., Song, H. H., Kim, Y.-B., & Cha, S. W. (2016). A thermally

self-sustaining solid oxide fuel cell system at ultra-low operating temperature (319°C). *Energy, 104*, 107–113.
12. Kwon, C. W., Lee, J. I., Kim, K. B., Lee, H. W., Lee, J. H., & Son, J. W. (2012). The thermomechanical stability of micro-solid oxide fuel cells fabricated on anodized aluminum oxide membranes. *Journal of Power Sources, 210*, 178–183.
13. Seo, H., Choi, Y., Koo, B., Jang, A., & Jung, W. (2016). Robust nano-architectured composite thin films for a low-temperature solid oxide fuel cell cathode. *Journal of Materials Chemistry A, 4*(24), 9394–9402.
14. Park, J., Lee, Y., Chang, I., Lee, W., & Cha, S. W. (2015). Engineering of the electrode structure of thin film solid oxide fuel cells. *Thin Solid Films, 584*, 125–129.
15. Ji, S., Chang, I., Lee, Y. H., Park, J., Paek, J. Y., Lee, M. H., & Cha, S. W. (2013). Fabrication of low-temperature solid oxide fuel cells with a nanothin protective layer by atomic layer deposition. *Nanoscale Research Letters*. https://doi.org/10.1186/1556-276X-8-48
16. Ji, S., Cho, G. Y., Yu, W., Su, P. C., Lee, M. H., & Cha, S. W. (2015). Plasma-enhanced atomic layer deposition of nanoscale yttria-stabilized zirconia electrolyte for solid oxide fuel cells with porous substrate. *ACS Applied Materials & Interfaces, 7*(5), 2998–3002.
17. Ji, S., & Tanveer, W. H. (2020). Thickness determination of porous Pt cathode thin film capped by atomic layer-deposited alumina for low-temperature solid oxide fuel cells. *Applied Surface Science, 514*, 145931.
18. Galinski, H., Ryll, T., Elser, P., Rupp, J. L. M., Bieberle-Hütter, A., & Gauckler, L. J. (2010). Agglomeration of Pt thin films on dielectric substrates. *Physical Review B, 82*(23), 235415.
19. Ji, S., Seo, H. G., Lee, S., Seo, J., Lee, Y., Tanveer, W. H., Cha, S. W., & Jung, W. (2017). Integrated design of a Ni thin-film electrode on a porous alumina template for affordable and high-performance low-temperature solid oxide fuel cells. *RSC Advances, 7*, 23600–23606.
20. Heintze, M., & Pietruszka, B. (2004). Plasma catalytic conversion of methane into syngas: The combined effect of discharge activation and catalysis. *Catalysis Today, 89*(1–2), 21–25.
21. Park, J. S., Holme, T. P., Shim, J. H., & Prinz, F. B. (2012). Improved oxygen surface exchange kinetics at grain boundaries in nanocrystalline yttria-stabilized zirconia. *MRS Communication, 2*(3), 107–111.
22. Chao, C. C., Kim, Y. B., & Prinz, F. B. (2009). Surface modification of yttria-stabilized zirconia electrolyte by atomic layer deposition. *Nano Letters, 9*(10), 3626–3628.
23. Cho, G. Y., Yu, W., Lee, Y. H., Lee, Y., Tanveer, W. H., Kim, Y., Lee, S., & Cha, S. W. (2020). Effects of nanoscale PEALD YSZ interlayer for AAO based thin film solid oxide fuel cells. *International Journal of Precision Engineering and Manufacturing-Green Technology, 7*, 423–430.
24. Huang, H., Nakamura, M., Su, P., Fasching, R., Saito, Y., & Prinz, F. B. (2007). High-performance ultrathin solid oxide fuel cells for low-temperature operation. *Journal of the Electrochemical Society, 154*(1), B20–B24.
25. Ji, S., Ha, J., Park, T., Kim, Y., Koo, B., Kim, Y. B., An, J., & Cha, S. W. (2016). Substrate-dependent growth of nanothin film solid oxide fuel cells toward cost-effective nanostructuring. *International Journal of Precision Engineering and Manufacturing-Green Technology, 3*(1), 35–39.

SangHoon Ji is currently working as Senior Researcher at Korea Institute of Civil Engineering and Building Technology. He received his doctorate in Intelligent Convergence Technology in 2015 from Seoul National University. His research interests include fuel cell material and system and hydrogen energy.

WeonJae Kim is currently working as Research Fellow at Korea Institute of Civil Engineering and Building Technology (KICT) and General Director of Department of Environmental Research at KICT. He received his doctorate in Urban Engineering in 2007 from University of Tokyo. His research interests include urban water and environmental resource recycling.